World Conference on Timber Engineering Oslo 2023

STUDY ON FAILURE MECHANISMS OF HYBRID STRUCTURE OF REINFORCED CONCRETE FRAME WITH CLT INFILL

Hamood Alwashali[1], Ahmad Ghazi Aljuhmani[2]

ABSTRACT: The objective of this study is to clarify the possible failure mechanisms and strength of RC frames with CLT infill, and to investigate the CLT panel compression strut width. Five failure mechanisms and a simplified strength evaluation method were proposed based on a literature review of the RC frames with different material infills. Experimental tests of diagonal compression of CLT panels were conducted and results were used in finite element analysis to evaluate the change of failure mechanisms based on strut width and relative stiffness for the RC frame and CLT.

KEYWORDS: Hybrid structures, Reinforced concrete buildings, CLT infill panels, Seismic capacity

1 INTRODUCTION

Hybrid reinforced concrete (RC) and timber structures are getting much attention, and their numbers are increasing rapidly as an eco-friendly solution to contribute towards the sustainable societies prescribed in the UN's Sustainable Development Goals (SDGs). Cross-laminated timber (CLT) has relatively high shear strength, is lightweight, and has low carbon emissions. Using CLT panels as shear walls in RC or steel structures can increase the seismic capacity of the building with also securing lower seismic demand due to CLT's low mass. In addition, CLT walls have relatively greater deformation capacity than RC shear walls, resulting in improving not only the lateral strength of the structure but also its ductility. However, the insertion of CLT panels in the RC frames could also lead to unwanted failure mechanisms (e.g., brittle failure). Therefore, it is essential to understand and investigate the possible failure mechanisms and seismic behaviour of these structures.

Recently in Japan, RC frames or steel frames with CLT infill buildings were constructed, as shown in Figure 1. Worldwide, several researchers have started investigating the effect of CLT infill on RC or steel frames. A parametric study on different types of steel frames with CLT infill using static pushover analysis was carried out by Dickof et al. [1] to clarify the ductility and overstrength values. It was found that CLT infill is effective in the case of lower ductility frames, whereas it does not have much influence in the case of ductile frames. [1] focused only on the influence of CLT infill on the ductility factor and the increase of strength for the RC frame. However, the possible failure mechanism, as well as an evaluation method, were not considered in [1]. Another numerical simulation has been carried out by Stazi et al. [2] to understand the effect of CLT infill on RC frames. This study also focused only on the overall influence of the CLT panel on the increase of the strength and stiffness of the RC frame. Several experiments on five 1/3 scale RC frames with different CLT infill types were conducted by Haba et al. [3]. In [3], even though several specimens with the same RC frame and different CLT panels' specifications were tested, only one failure was observed, which is a shear failure in the RC columns. As for Steel structures with CLT infill, there have been few recently constructed buildings in Japan [4] and several experiments tested by Fukumoto et al. [5]. However, there is a lack of research on RC buildings with CLT shear walls, and in the previous studies[1-3], researchers have only investigated the increase in strength and ductility of the frame due to the insertion of the CLT panel. In addition, research on the different possible failure mechanisms of such structures is still lacking, and evaluation guidelines and standards for engineering practice are still unavailable.

Therefore, the objectives of this study are: first, clarify the possible in-plane failure mechanisms of RC frames with CLT panels infill. Finally, Investigate the effect of different parameters (e.g., compression strut width and CLT-to-RC connections) on the expected failures.

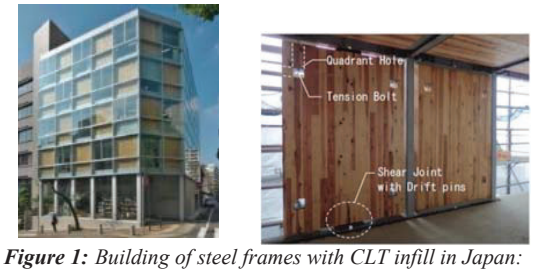

Figure 1: *Building of steel frames with CLT infill in Japan: Hyogo Forestry Hall [4](left figure). Details of CLT panel with steel frame (right figure) [5]*

[1] Hamood Alwashali, Okayama University, Japan, hamood@okayama-u.ac.jp
[2] Ahmed Ghazi Aljuhmani, Tohoku University, Japan, aljehmani@rcl.archi.tohoku.ac.jp

https://doi.org/10.52202/069179-0431

2 EXPECTED FAILURE MECHANISMS

Although CLT Infill in RC frames is a new concept, infill walls or post-installed walls are common practices, such as masonry infill walls and steel braces. The main difference is that the material properties of the CLT panel are different, which may completely alter the RC frame performance compared to other conventional methods, and this has not been investigated in past studies. Possible failure mechanisms and evaluation methods of lateral strength capacity were investigated. In this section, the possible failure mechanisms of RC frames with CLT infill systems are investigated based on previous research or based on comparisons with other infill materials.

2.1 COLUMN SHEAR FAILURE

This failure was observed in experiments by Haba et al. [1] and is shown in Figure 2 and illustrated in Figure 3. 1/3 scale specimen with CLT panels along the entire width of the frame (1540 mm) was tested. The height of the CLT infill was 840 mm, and it was fixed with the RC frame using epoxy resin. Two panels of Japanese Cedar CLT (Mx60b-3-3 grade) were used with 60 mm thickness (30 mm for each panel). In this case, the RC columns are shear-critical columns (the shear capacity for the RC columns is less than the flexural capacity). Thus, the frame does not have enough deformation capacity for the CLT infill to fail first, and the dominant failure will be column shear failure.

In this case, A simple estimation of the maximum strength capacity is proposed to be calculated by adding three components: the strength of the two RC columns and the strength of connections at the top of the CLT panel, and is shown in Equation (1), with reference to Figure 3.

$$Q_{sh} = 2 \times Q_{su} + Q_{joint} \quad (1)$$

Where Q_{su} is the column shear strength calculated as prescribed in the Japanese AIJ code [6], or it can be calculated using any other adequate standards or method. The Q_{joint} is the strength of the CLT to RC joint on top, in the test by [1], it was estimated using the strength of the epoxy material injected between the RC frame and CLT infill. If there are no connections between the CLT panel and the RC frame, then Q_{joint} can be ignored.

Figure 2: *Column shear failure as observed in [3]*

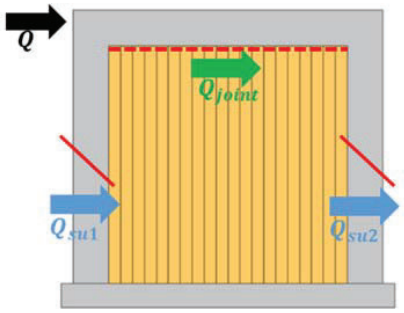

Figure 3: *Column shear failure for RC frame with CLT*

2.2 PUNCHING SHEAR FAILURE

Having relatively strong and very stiff walls within an RC frame could cause a punching shear failure, which is observed in RC frames with strong steel braces as in Ishimura et al. [7], as shown in Figure 4 and in Figure 5 in Japanese seismic evaluation standard JBDPA [8]. Punching shear failure of RC frame is also observed with other types of infill walls such as masonry infill that were retrofitted by ferrocement, mentioned by Sen et al. [9]. This failure could happen in the case of a very strong CLT infill relative to the surrounding RC frame.

In this case, maximum strength capacity can be estimated by adding three components. The first component is the RC column (windward) which has punching shear failure. The second component is the connections at the top of the CLT panel and RC beam. The third component is the leeward RC column, which could fail in either shear or flexural, and can be calculated by Equation (2), with reference to Figure 6.

$$Q_{pun} = PQ_{c1} + Q_{joint} + min(Q_{su}, Q_{mu}) \quad (2)$$

Where PQ_{c1} is the punching shear capacity of the first column as prescribed in JBDPA [8], Q_{su} is column shear strength, and Q_{mu} is column flexural strength.

Figure 4: *Punching shear failure as observed in [7]*

https://doi.org/10.52202/069179-0431

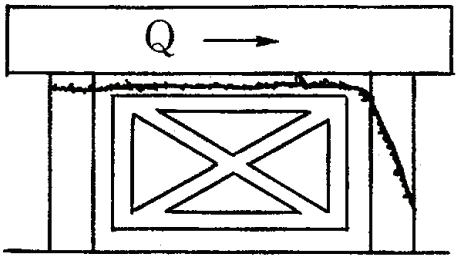

Figure 5: *Punching shear failure illustrated in JBDPA [8]*

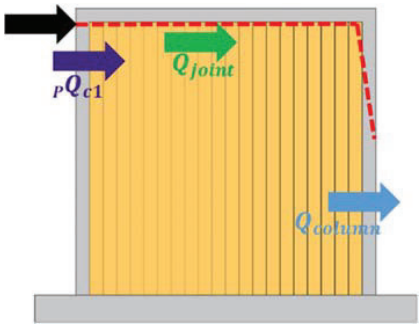

Figure 6: *Punching shear failure for RC frame with CLT*

2.3 FRAME OVERALL FLEXURAL FAILURE

Figure 7 shows the overall flexural failure that could occur when the CLT infill is stiff relative to the RC frame and the CLT panel is strongly connected to the RC frame.

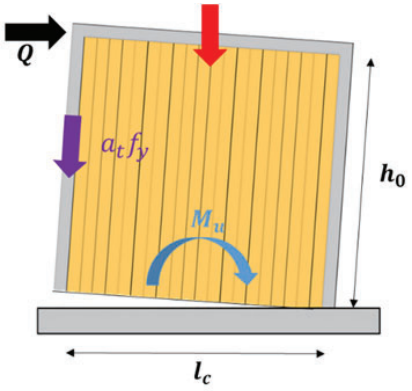

Figure 7: *overall flexural failure of the composite structure*

In this case, the RC frame and CLT panel will act as a single component similar to a cantilever flexural wall. There are no experimental tests of RC frames with CLT infill having an overall flexural failure. However, similar behaviour is observed with other infilled walls, such as tests by Laughery et al. [10] on RC frames with post-installed RC walls shown in Figure 8. It can occur as well with masonry infills such as tests by Sen et al. [9]. In this failure, maximum strength capacity can be estimated by the overall flexural capacity (Q_{fl}) as a cantilever flexural wall as shown in Figure 8. The maximum strength could be calculated using Eq. 3 and Eq. 4 which are adopted from JBDPA [8] with reference to Fig.7.

$$Q_{fl} = M_u / h_0 \quad (3)$$

$$M_u = a_t f_y l_c + 0.5 N l_c \quad (4)$$

Where M_u is moment capacity, h_0 is the clear height of the column, a_t is longitudinal reinforcement area for one column, f_y is the yield strength of the column's longitudinal reinforcement, l_c is the distance between the centers of the boundary columns, and N is the total axial load applied on the entire frame. It should be noted here that the maximum strength is calculated entirely based on the RC frame strength. There is no contribution for the CLT panel by assuming there are no tension connections between the CLT panel and the RC frame at the bottom. If connections are added at the bottom of the CLT panel, then the tensile of the CLT panel could also contribute to the flexural capacity and need to be added to Eq. 4.

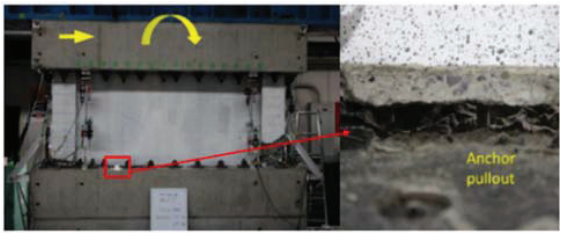

Figure 8: *Overall flexural failure as observed in [10]*

2.4 CLT PANEL SHEAR FAILURE

No experimental studies are showing the shear failure of CLT walls in RC frames. However, other infill materials such as masonry infill walls in RC frames had a shear failure, such as those shown in Figure 9. For CLT infill, it could occur in a ductile RC frame with relatively lower stiffness for CLT. In this case, the columns are flexural columns (the flexural capacity of the column is less than the shear capacity of the column). Thus, the frame has enough deformation capacity for the CLT infill to deform, and the dominant failure will be CLT failure. Capacity can be calculated by adding the flexural strength of the two columns to the shear strength of the CLT panel itself, as shown in Equation (6) and Equation (7) with reference to Figure 10. It should be noted here that Q_{mu} needs to be calculated assuming the clear height h_0 to be around half of the column clear height.

$$Q_{CLT-s} = Q_{mu1} + Q_{mu2} + S_{CLT} \quad (6)$$

$$S_{CLT} = \tau_{CLT} \times L_{CLT} \times t_{CLT} \quad (7)$$

Where Q_{mu1} and Q_{mu2} are windward and leeward column capacity, S_{CLT} is CLT panel shear capacity, and τ_{CLT}, L_{CLT}, and t_{CLT} are CLT panel shear strength, length, and thickness, respectively.

https://doi.org/10.52202/069179-0431

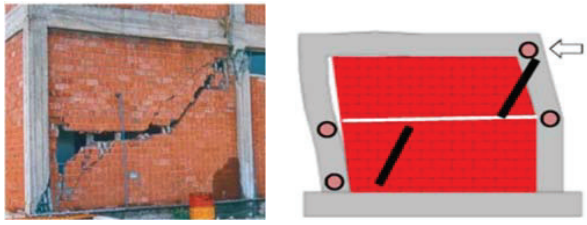

Figure 9: *Masonry shear failure in 1999 Turkey EQ (left figure) [11], and as observed in Sen et al. [9] (right figure)*

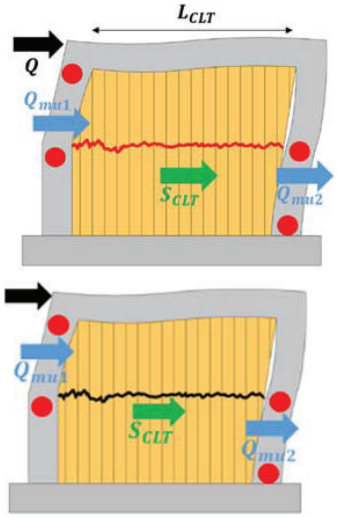

Figure 10: *CLT shear failure for RC with CLT infill*

2.5 CLT PANEL COMPRESSION FAILURE

There are no experimental studies yet showing the failure of CLT diagonal compression failure in RC frames but there are recent tests of steel frames with CLT infill such as experimental tests by Fukumoto et al. [5] and shown in Figure 11. However, Fukumoto`s tests are of steel frames without any boundary columns attached to CLT infill as shown in Figure 11, which is different from the concept investigated here of RC frames confining the CLT infill. In addition, other infill materials in RC frames, such as masonry walls, had a shear failure considering diagonal compression failure, which was observed in the experiment done by Alwashali et al. [12] on masonry infill, as shown in Figure 12. It is thought that CLT infill could also have a similar failure mechanism.

This failure is similar to the CLT panel shear failure; however, in this case, CLT compression capacity (C_{CLT}) is less than CLT shear capacity (S_{CLT}).

This failure capacity can be calculated by Equation (8) and Equation (9) with reference to Figure 13.

$$Q_{CLT-c} = Q_{mu1} + Q_{mu2} + C_{CLT} \quad (8)$$

$$C_{CLT} = \sigma_{CLT} \times W_{strut} \times t_{CLT} \times \cos\theta \quad (9)$$

Where C_{CLT} is CLT panel shear capacity, σ_{CLT} is CLT panel compressive strength, W_s is compression strut width with, θ is the angle between the RC base and the strut with reference to Figure 13. The estimation of the strut width (W_s) is a complex topic that has not been studied previously for CLT infills. The following section will investigate the strut width based on simple diagonal compression tests and finite element analysis.

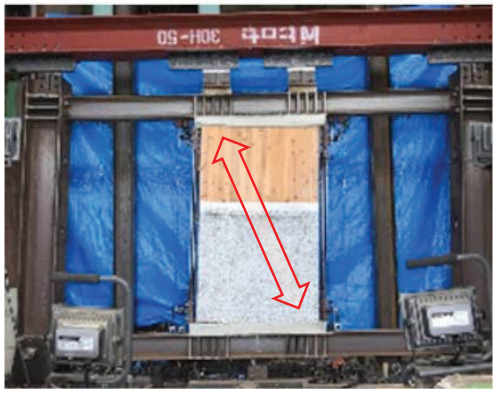

Figure 11: *Experiments of Steel frame with CLT infill tested by Fukumoto et al. [5]*

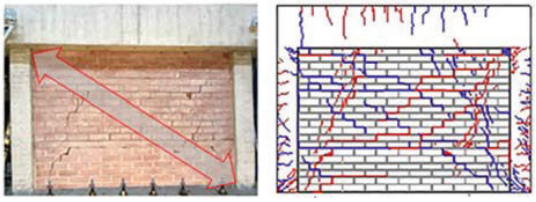

Figure 12: *Compression strut failure of RC frame with masonry infill [12]*

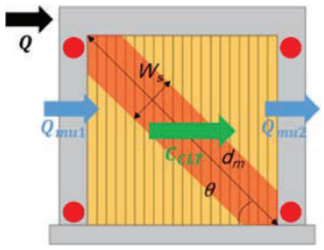

Figure 13: *overall flexural failure of the composite structure*

3 COMPRESSION STRUT MECHANISM

The capacity evaluation for all the failure mechanisms mentioned above, except CLT compression strut failure, is relatively well understood and thought that could be directly applied. However, the failure of the compression strut of CLT infill as well as its width is still poorly understood. Thus, in this section, we investigated the strut width based on conducting diagonal compression tests on CLT walls and then model the CLT infill using finite element analysis to investigate the strut width.

https://doi.org/10.52202/069179-0431

3.1 DIAGONAL COMPRESSION STRUT

In the case of CLT infill, no calculation approaches nor empirical equations were proposed for strut width. One simple approach is to assume the methods used for masonry infill might also be applicable to CLT infill. In this study, the two methods by FEMA-306 [13] and Sen et al. [9] only are compared. The values of strut width to the diagonal length that are calculated by the two methods for different flexural relative stiffness (frame flexural stiffness divided by CLT panel flexural stiffness) are shown in Figure 13. The calculations of strut width by [9] and [13] showed large variations, as can be seen in Figure 14. This could lead to uncertainty in estimating strength by the failure mechanism of the strut.

In order to adequately estimate the strut width of CLT infill in the RC frame, simple diagonal tests were conducted, and then finite element models were developed and validated by the diagonal test. The FE analysis is then used to simulate the CLT infill in the RC frame to estimate the compression strut width.

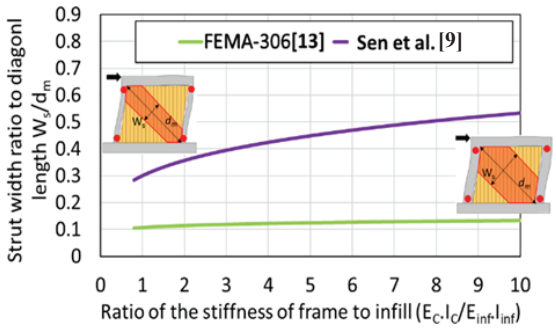

Figure 14: *Strut width relation with relative flexural stiffness of RC frame to CLT infill*

3.2 DIAGONAL COMPRESSION EXPRIMENT

The interaction between the CLT infill panel and the RC frame under lateral forces is shown in Figure 15. The transmitted forces to the CLT panel at the corner of the actual RC frame could be reproduced using a diagonal compression test configuration, as shown in Figure 15. Therefore, this test-set up was used to obtain the characteristics of CLT panels under compression forces.

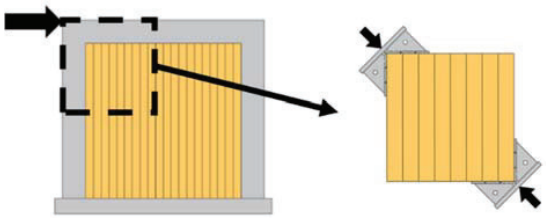

Figure 15: *Behaviour of CLT panel under lateral load*

A hydraulic Jack was used to apply a monotonic vertical downwards force on a 1200 mm by 1200 mm CLT panel (loading rate in the range of 0.15~0.2 mm/s). Three replicates were tested, and all the panels were 5-layer 150 mm thick panels made from Japanese cedar with Mx-60-5-5 grade. Each panel was installed vertically between two steel 'shoe' caps as shown in Figure 16 and Figure 17, which were designed to distribute the load such that local bearing failure of the CLT panel does not occur.

LVDTs were attached along the two diagonals of the CLT panel to calculate shear deformation. Shear deformation was calculated using Equation (10) with reference to Figure 18.

$$\gamma = \frac{\Delta x + \Delta y}{900 \times \sqrt{2}} \qquad (10)$$
$$\delta = \gamma \times 1200$$

Where Δx and Δy are the values obtained from the horizontal and the vertical overall LVDTs, respectively.

In addition, digital image correlation (DIC) was also used in the tests and the properties and details of the DIC setup are shown in Figure 19, and data were analyzed using the DIC Software OPTECAL [14].

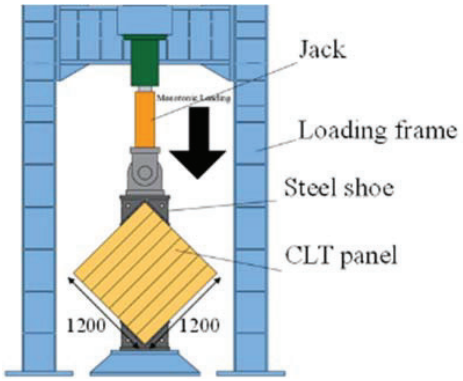

Figure 16: *Loading set-up of the compression test*

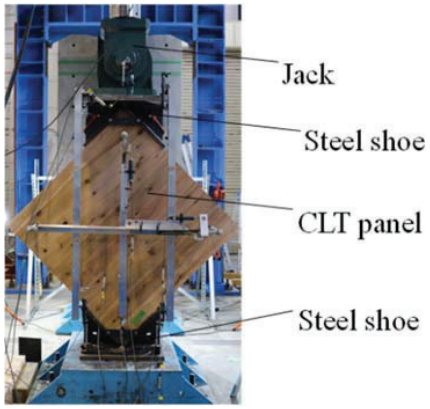

Figure 17: *photo of Loading set-up of the test*

https://doi.org/10.52202/069179-0431

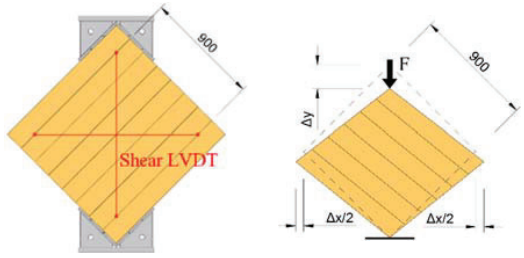

Figure 18: *LVDTs set-up and shear deformation*

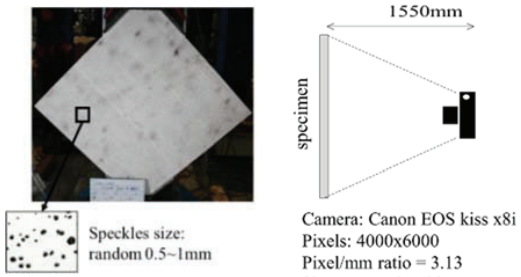

a) The painted side of the specimen for DIC

b) Location of the camera

Figure 19: *The details of the DIC set-up*

3.3 SIMULATION USING FEM MODEL

A numerical model was created using the FEM software Abaqus [15]. The CLT panel was modelled as a solid element. The model consists of five layers, and the interaction between each CLT layer was assumed to be a tie constraint with no slip. Each layer was modelled as an elastic orthotropic material with three directions (L, R, T): longitudinal (in the direction of the grain), radial, and tangential as shown in Figure 20. Each CLT layer has an axis orientation perpendicular to the adjacent layers. The mechanical properties of each layer are shown in Table 1, which was taken from the Japanese Wood Handbook [16].

Table 1: *Japanese Cedar material properties [16]*

Species	Young modulus (MPa)			Shear modulus (MPa)			Poisson ratio		
	E_L	E_R	E_T	G_{LT}	G_{LR}	G_{RT}	ν_{LT}	ν_{LR}	ν_{RT}
Japanese cedar	8700	620	260	460	650	15	0.58	0.405	0.901

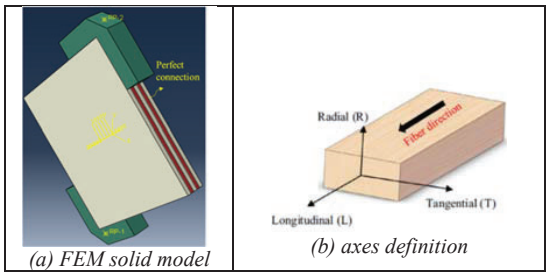

(a) FEM solid model

(b) axes definition

Figure 20: *CLT panel FEM model properties*

A comparison between shear displacement-shear force curves for the FE model and experiment is shown in Figure 21. The stiffness obtained from the FE model (100.4 kN/mm) was relatively close values to the average value from the experiment (106.3 kN/mm).

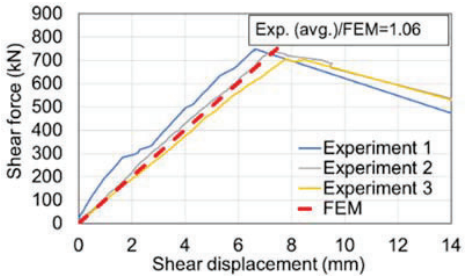

Figure 21: *Comparison between FEM and experiments*

A comparison between the strain obtained from the experiment by DIC and FEM results is shown in Figure 22. In this case, horizontal (ε_x) and vertical (ε_y) axial strain distribution were compared at the point just before maximum load P_{max}. Overall, the strain distribution is

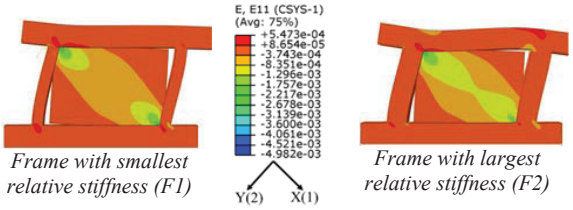

Frame with smallest relative stiffness (F1)

Frame with largest relative stiffness (F2)

similar in both FEM and DIC, showing that the response is governed by one main compressive strut, indicating that FEM can capture the general stress paths and give close strain values.

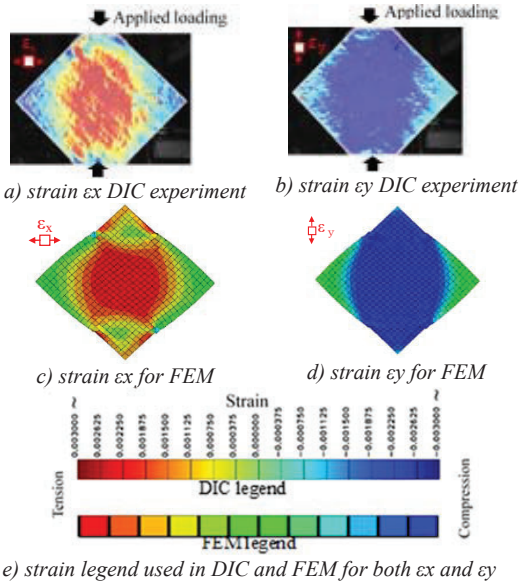

a) strain εx DIC experiment

b) strain εy DIC experiment

c) strain εx for FEM

d) strain εy for FEM

e) strain legend used in DIC and FEM for both εx and εy

Figure 22: *Comparison between FEM and DIC*

https://doi.org/10.52202/069179-0431

3.4 FEM MODEL FOR RC FRAME WITH CLT INFILL

FEM software Abaqus [15] was used to model the RC frame with CLT infill. Only concrete was modeled with elastic solid elements for simplicity, since the main focus is the strut width in the CLT infill. Young's modulus and Poisson's ratio for RC were taken as 23000 MPa and 0.2, respectively. The CLT model was the same as the model used in the diagonal compression model (section 3.3). The frame was fixed in all directions at the bottom and free at the top. The interaction between the CLT panel and the RC frame was assumed as hard contact with no penetration between the CLT and RC elements with no friction interaction. A total of 10 frames was modelled, and the difference between each model is the relative flexural stiffness between the RC columns and the CLT infill (infill thickness was fixed, and the RC columns' dimensions were increased).

Regarding stiffness increase due to the CLT infill, the initial stiffness of bare frame F1 (the frame with the smallest relative stiffness) was 17.5 kN/mm, and stiffness increased to 75.4 kN/mm after adding the CLT infill with an increase of about 4.3 times. The initial stiffness of bare frame F2 (the frame with the largest relative stiffness) was 121.9 kN/mm, and stiffness increased to 185.9 kN/mm after adding the CLT infill with an increase of about 1.5 times. The results of strain in the diagonal strut direction for the F1 frame and F2 frame are shown in Figure 23. Although the strain values differ slightly between these two frames, the strut width almost does not vary much. In order to compare quantitative values of the strut width, a method proposed by Jin et al. [17] was used. In this FEM analysis, a total of 12 sections were taken, and, for each section, the average strain was calculated by taking the equivalent strain area for the actual strain curve as shown in Figure 24.

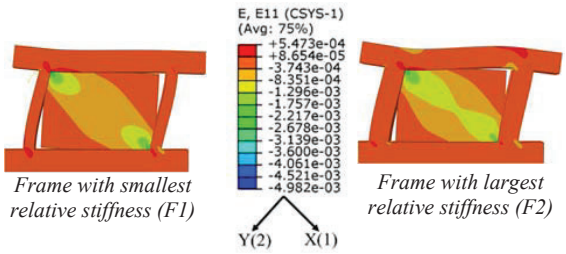

Figure 23: *Normal strain in X-direction (strut direction)*

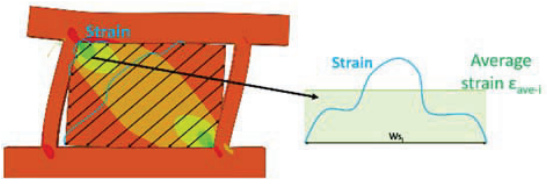

Figure 24: *Strut sections and average strain calculations*

The strut width obtained from the FEM analysis for different relative RC to CLT stiffness is shown in Figure 25. In Figure 25, The strut width ranges between $0.34d_m$ and $0.36d_m$ with different relative RC to CLT stiffness. When also compared to the two masonry infill methods [9,13], it was found that FEM analysis has a similar tendency with FEMA-306 [13] for masonry infill; however, FEM analysis gave larger strut width values.

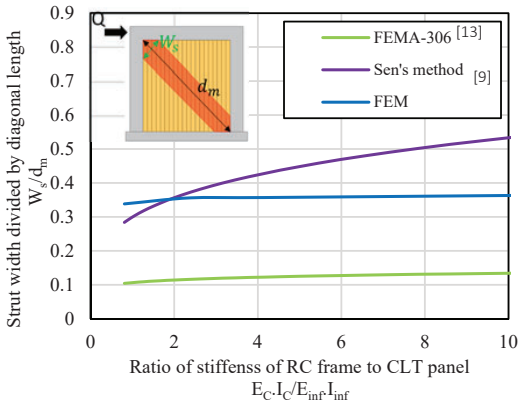

Figure 25: *Comparison of strut width obtained by FEM modelling CLT versus other methods*

3.5 EXAMPLE OF STRENGTH EVALUATION

In this study, the lateral strength of the RC frame with CLT infilled (Q_{cal}) is proposed to be calculated by taking the minimum of the calculated lateral capacity based on the five different failure mechanisms discussed previously in section 2, as shown in Equation (11).

$$Q_{cal} = min(Q_{sh}, Q_{pun}, Q_{fl}, Q_{CLT-c}, Q_{CLT-s}) \qquad (11)$$

A case study of the RC frame tested by Alwashali et al. [12] with masonry infill (specimen F-1.5) will be presented to understand the failure mechanisms well. This RC frame will be used here, assuming CLT infill as shown in Figure 26. The thickness of the CLT panel is assumed to be 60 mm, and shear and compression strength for CLT are assumed to be 4.1 MPa and 174 MPa, respectively. These values are based on the material tests conducted based on the diagonal compression test presented in section 3.2.

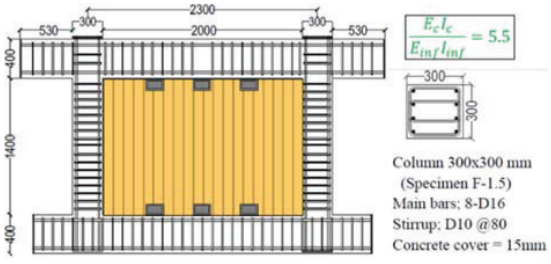

Figure 26: *A case study on RC frame for capacity evaluation (from Alwashali et al. [12])*

https://doi.org/10.52202/069179-0431

A comparison between several methods for only the compression failure strength of the case study frame is shown in Figure 27. It should be noted that deformation capacity evaluation is out of the scope of this paper and thus the story drift axis in Figure 27 and Figure 28 is used for illustration only. As shown in Figure 27, there is a large variation between the estimation of maximum strength for the diagonal compression failure considering previous studies for different materials. The FE analysis investigated in this study gives around 2 times (1037kN) the value estimated using the FEMA 306 method (548kN). This uncertainty and the lack of CLT strut width experiments will lead to significant variations in the expected strength capacity and failure mechanisms.

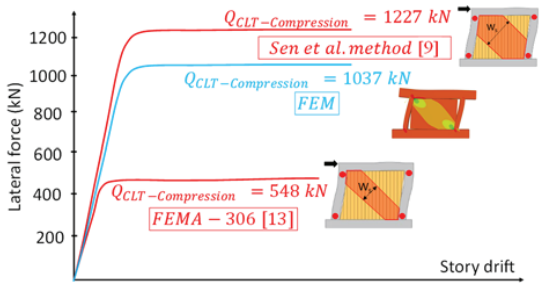

Figure 27: *Failure strength for the case study frame*

The expected lateral strength capacity of the case study frame for all the five expected failure mechanisms is as shown in Figure 28.

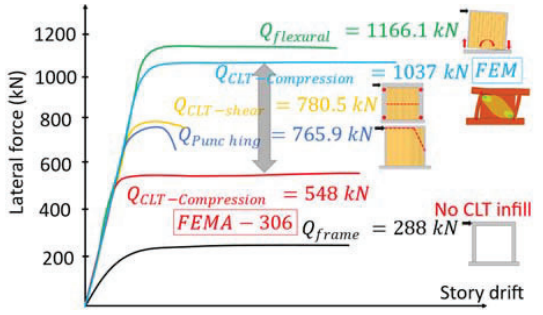

Figure 28: *Calculated capacity of the case study frame*

Three shear connections were assumed at the top and at the bottom of the CLT infill to make the example shown here more practical. This number was also assumed to avoid punching shear failure. Each shear connection has a shear strength of 80 kN (total of 240 kN as Q_{joint} in Eq(2). For CLT compression strut failure, the FEMA 306 [13] (for masonry) and FE analysis results (presented in this study) were used to calculate the strut width. As shown in Figure 28, compression failure gives the minimum strength value and is expected in a case assuming the strut width of masonry as in FEMA-306 [13]. However, in the case of strut width obtained from the FE analysis, the capacity of compression failure increased, and thus punching shear failure becomes the most probable failure type. The influence of the strut width is crucial in seismic design since it affects not only the maximum capacity but also the expected seismic behaviour, which could change the behaviour from desirable ductile failure to undesirable brittle punching shear failure. Experimental verification and investigation to understand the behaviour of CLT infills are still needed.

4 CONCLUSIONS

This study presented different expected failure modes for hybrid structures of Reinforced concrete (RC) frames with CLT infill based on previous studies and observations for RC frames with other infills. Also, a FEM model was developed and verified by component compression test to study the effect of CLT compression strut width on the expected failure. The main conclusions are as follows:

1. Five different possible failure modes for RC frames with CLT infill were studied based on the literature review for RC frames with other material infills.
2. The seismic capacity and in-plane failure mechanism of RC frames with CLT infill could be predicted based on the evaluation method presented in this paper.
3. Compression strut width methods for RC frames with masonry infill have big variations when used with CLT.
4. FEM analysis showed that the compression strut width does not change much by changing the relative stiffness of the RC frame and the CLT infill (the margin was between 0.34 and 0.36 of the strut length).
5. CLT compression strut width and CLT-to-RC shear connections could significantly affect the probable failure mechanisms, changing it from ductile to brittle failure. Therefore, further experimental investigations are needed to predict the probable failure mechanism.

ACKNOWLEDGEMENT

The study was partly supported by the agency of Japan Society for the Promotion of Science (JSPS) and project KAKENHI Grant Number 21K14283 (Principal investigator: Hamood Alwashali, Okayama University).

REFERENCES

[1] Dickof, C., Stiemer, S.F., Bezabeh, M.A. and Tesfamariam, S., 2014. CLT–steel hybrid system: Ductility and overstrength values based on static pushover analysis. Journal of Performance of Constructed Facilities, 28(6), p.A4014012.

[2] Stazi, F., Serpilli, M., Maracchini, G. and Pavone, A., 2019. An experimental and numerical study on CLT panels used as infill shear walls for RC buildings retrofit. Construction and building materials, 211, pp.605-616.

[3] Haba, R., Kitamori, A., Mori, T., and Fukuhara, T., 2016. Development of clt panels bond-in method for seismic retrofitting of RC frame structure. J. Struct. Constr. Eng, 81, pp.1299-1308.
[4] Xtech 2019, accessed 30 December 2021, <https://xtech.nikkei.com/atcl/nxt/mag/na/18/00076/100200003/>.
[5] Fukumoto K., Kouda M., Kubo K., Usami T., Kitamori A., Miyauchi Y., and Isoda H., 2021 Experimental study on CLT seismic panel infilled within steel frame. J. Struct. Constr. Eng., AIJ, Vol. 86, No.787, 1345-1356, Sep., 2021
[6] AIJ, 2016. AIJ Standard for Lateral Load‐Carrying Capacity Calculation of Reinforced Concrete Structures.
[7] Ishimura, M., Sadasue, K., Miyauchi, Y., and Yokoyama, T., 2012, September. Seismic performance evaluation for retrofitting steel brace of existing RC building with low-strength concrete. In Proc. of the 15th World Conf. on Earthquake Engineering, 15th WCEE (pp. 24-28).
[8] JBDPA/The Japan Building Disaster Prevention Association, 2001. Standard for seismic evaluation of existing reinforced concrete buildings.
[9] Sen, D., Alwashali, H., Tafheem, Z., Islam, M. S., and Maeda, M., 2020, September. Experimental investigation and capacity evaluation of Ferro-cement laminated masonry infilled RC frame. In Proc. of the 17th WCEE.
[10] Laughery, L., Ichinose, T., Maeda, M., Alwashali, H., Takahashi, H., Hanzawa, M., Okada, T., Ide, A. And Sonn, K., A Potential Vulnerability In High-Strength Reinforced Concrete Shear Wall Retrofits.
[11] Bachmann, H. and Suisse. Office fédéral de l'environnement, 2003. Seismic conceptual design of buildings: basic principles for engineers, architects, building owners, and authorities. SDC.
[12] Alwashali, H., and Sen, D., 2019. Experimental investigation of influences of several parameters on seismic capacity of masonry infilled reinforced concrete frame. Engineering Structures, 189.
[13] Federal Emergency Management Agency, 2013. Evaluation of earthquake damaged concrete and masonry wall buildings. FEMA.
[14] Optical: Digital Image Correlation software 2020.
[15] Dassault Systemes Simulia Corp., Abaqus software.
[16] Basic theory of wood structure: Architectural Institute of Japan: Wood Industry Handbook.
[17] Jin, K., Choi, H. and Nakano, Y., 2016. Experimental study on lateral strength evaluation of unreinforced masonry-infilled RC frame. Earthquake Spectra, 32(3), pp.1725-1747.

https://doi.org/10.52202/069179-0431